Electronic Structure of Germanium Monohydrides Ge_nH, $n = 1-3$

G. Gopakumar,[†] Vu Thi Ngan,[†] Peter Lievens,[‡] and Minh Tho Nguyen*[,†]

Department of Chemistry, Laboratory of Solid State Physics and Magnetism, and Institute for Nanoscale Physics and Chemistry (INPAC), University of Leuven, B-3001 Leuven, Belgium

Received: June 12, 2008; Revised Manuscript Received: September 16, 2008

Quantum chemical calculations were applied to investigate the electronic structure of germanium hydrides, Ge_nH ($n = 1, 2, 3$), their cations, and anions. Computations using a multiconfigurational quasi-degenerate perturbation approach (MCQDPT2) based on complete active space wave functions (CASSCF), multireference perturbation theory (MRMP2), and density functional theory reveal that Ge_2H has a $^2B_1$ ground state with a doublet-quartet gap of ~39 kcal/mol. A quasidegenerate $^2A_1$ state has been derived to be 2 kcal/mol above the ground state (MCQDPT2/aug-cc-pVTZ). In the case of the cation Ge_3H^+ and anion Ge_3H^-, singlet low-lying electronic states are derived, that is, $^1A'$ and $^1A_1$, respectively. The singlet−triplet energy gap is estimated to 6 kcal/mol for the cation. An "Atoms in Molecules" (AIM) analysis shows a certain positive charge on the Ge_n ($n = 1, 2, 3$) unit in its hydrides, in accordance with the NBO analysis. The topologies of the electron density of the germanium hydrides are different from that of the lithium-doped counterparts. On the basis of our electron localization function (ELF) analysis, the Ge−H bond in Ge_2H is characterized as a three-center-two-electron bond. Some key thermochemical parameters of Ge_nH have also been derived.

Introduction

Germanium thin films have been potential materials in the semiconductor industry for many years. The primary application of germanium (Ge), which is isovalent with carbon and silicon, is in transistor elements. The deposition of Ge layers is generally achieved by chemical vapor deposition (CVD) mainly using germane (GeH_4).[1] Besides these industrial applications, germanium hydrides are also interesting from a fundamental point of view. A number of Ge_nH_m species have been a subject of both experimental and theoretical investigations. Many of these studies concentrated on their structure[2] and reactivity[3] including the ionic clusters.[4] The heats of formation of GeH_n and Ge_2H_n were predicted by Ricca and Bauschlicher,[5] whereas the Ge_2H_m ($m = 0-5$) were examined by Antoniotti et al.[6] using DFT methods. Recently, the electronic structure of Ge_2H fragment was revisited by Wang et al.[7] at the coupled-cluster CCSD(T) level. In a nearly parallel study, Koizumi et al.[8] reconsidered the heat of formation of GeH_4 fragment at the CCSD(T) level with energy extrapolated to the complete basis set limit (CBS).

The continuing interest in small elemental and molecular aggregates extends to the clusters of germanium, and this is anticipated due to their possible role in surface growth processes and potential new applications in nanoelectronics.[9,10] Experimental studies on small germanium clusters started in 1954 when Ge_n clusters containing two to eight atoms were first detected by Kohl.[11] Since then, a number of both experimental[12−18] and theoretical[19−26] studies were reported. Knowledge about the structural and electronic identity of a cluster is important as its properties, specifically, thermodynamic stability, are inherently dependent on it. Because of such reason, most reported investigations focused on their geometries and some other energetic parameters such as dissociation energies and electron affinities.

Recently, our effort has been dedicated to the characterization of metal-doped Ge_n clusters.[27−29] Dopant atoms such as lithium or chromium have thus been found to exert large effects on the shape and properties of clusters. On the other hand, the nature of the interaction between Ge clusters with small molecules and radicals is also of significant interest, as this allows us to probe the cluster reactivities as potential catalysts. Let us consider the hydrogen atom as the simplest interacting moiety. It is important to know how and at which position H is bonded. In this context, we set out to pursue the study investigating the electronic and energetic properties of the simplest germanium monohydrides Ge_nH, with $n = 1$, 2, and 3, using ab initio molecular orbital and density functional theory computations. In our recent studies,[26−29] we have investigated in detail the simplest bare Ge_2 and Ge_3 forms. For the sake of consistency, we used the same theoretical approaches to determine the key geometrical and thermochemical parameters of Ge_nH. The nature of the Ge−H bonding was also further characterized by a partition of the electron density.

Methods of Calculations

Our computations involved density functional theory (DFT) using the popular B3LYP functional in conjunction with the 6-311++G(d,p) basis set. As a preliminary step, the geometry optimizations were performed and followed by harmonic vibrational frequency analysis at the aforementioned level. The DFT computations were refined with the help of ab initio molecular orbital theory calculations, where a complete active space self-consistent-field (CASSCF) method was applied. For MO computations, we used the larger correlation consistent aug-cc-pVTZ basis set to improve the accuracy. Given the fact that this method usually corrects for nondynamical or quasidegenerate correlation effects within the active space, the evaluation of dynamical correlation energies is, indeed, necessary for the description of states having multiconfigurational character.[30] For this purpose, we performed a perturbation analysis at the multiconfigurational level, using the multiconfigurational quasi-

* Corresponding author. Fax: 32-16-32 7992. E-mail: minh.nguyen@chem.kuleuven.be.
[†] Department of Chemistry and INPAC.
[‡] Laboratory of Solid State Physics and Magnetism and INPAC.

10.1021/jp805173n CCC: $40.75
Published on Web 11/06/2008

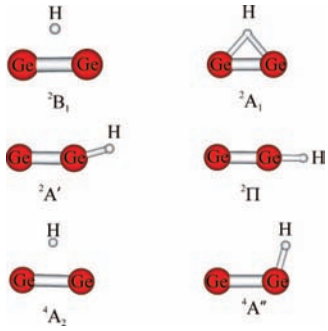

Figure 1. CASSCF(9,9)/aug-cc-pVTZ optimized geometries for various low-lying electronic states of Ge_2H.

degenerate perturbation theory (MCQDPT2)[31] and the more popular multireference second-order perturbation theory (MRMP2)[32] method. The former method usually provides corrected energies at second order for all states included in the model space simultaneously.[27,28] Throughout our MCQDPT2 analysis, an intruder-state-free technique has been adopted using a small energy denominator shift value to correct the "intruder states" problem.[33] However, for the Ge_3H system, the geometry optimizations were performed at the coupled cluster CCSD(T) level in conjunction with the aug-cc-pVDZ basis set. Single point computations were performed on these geometries employing the larger aug-cc-pVTZ and aug-cc-pVQZ basis set to further characterize the energetics of the lowest-lying electronic states. The electronic structure of the Ge_nH considered is discussed in the following sections, and, as a final step, an atoms-in-molecules (AIM) and electron localization function (ELF) analysis was performed for additional insights. All computations, reported hereafter, were performed using the Gaussian 03 revision D02,[34] GAMESS,[35] AIM2000,[36] BADER,[37] and TopMod[38] suites of programs.

Results and Discussion

A. GeH, GeH^+, and GeH^-. There has been a considerable interest in GeH. In the most recent theoretical study, Li et al.[39] carried out a systematic analysis on GeH_n ($n = 0-4$) using five different density functionals. In agreement with their results, we derived a $^2\Pi$ ground electronic state for GeH at the CASSCF/aug-cc-pVTZ level. For CASSCF computations, the 4s and 4p orbitals of Ge and the 1s orbitals of H are included in the active space, thus leading to a 5 electrons in 5 orbitals active space, referred to hereafter as CASSCF(5,5). The shape of the five active orbitals is illustrated in Figure 1. Here, the molecular axis is taken as the z-axis. The total energies computed at the CASSCF and two different perturbation levels, MRMP2 and MCQDPT2, are listed in Table 1.

The experimental value for the bond length of neutral GeH is 1.589 Å[40] obtained from microwave spectroscopy. In the previous investigation,[39] the most accurate theoretical comparison was achieved with the BHLYP functional in conjunction with a double ζ plus polarization (DZP) basis set augmented with s and p diffuse functions. Our CASSCF/aug-cc-pVTZ computations predicted a GeH bond length of 1.617 Å, overestimating the experimental value by 0.028 Å. The leading electronic configuration for the ground state of GeH has been derived as X $^2\Pi$:...$(1\sigma)^2(2\sigma)^2(1\pi_x)^1$. The unpaired electron occupies the π molecular orbital, which is mainly one of the degenerate p(Ge) orbitals. A low-lying quartet $^4\Sigma$ state with a leading electronic configuration $^4\Sigma$:...$(1\sigma)^2(2\sigma)^1(1\pi_x)^1(1\pi_y)^1$ has also been derived, which is energetically located at 36 kcal/mol above the ground state (CASSCF/aug-cc-pVTZ). The doublet to quartet excitation is initiated by promotion of an electron from the completely filled 2σ MO of the former to the degenerate $1\pi_y$ MO of the latter. The GeH($^4\Sigma$) bond length of 1.562 Å is shorter as compared to that of the $^2\Pi$ state, because electron excitation occurs from the Ge−H antibonding 2σ-MO. Incorporating the dynamical correlation energy, we evaluated the doublet−quartet gap at two different perturbation levels, MRMP2 and MCQDPT2, which amounts to 38 and 39 kcal/mol, respectively. It should be noted that the B3LYP functional overestimates the gap to 49 kcal/mol, irrespective of the basis set employed.

Removal of an electron results in the formation of GeH^+ cation for which a closed-shell singlet ground $^1\Sigma^+$ state has been derived. The leading electronic configuration of the CASSCF (4,5) wave function is $^1\Sigma^+$:...$(1\sigma)^2(2\sigma)^2(1\pi_x)^0$ corresponding to removal of an electron from the π-MO. A triplet $^3\Pi$ state with the dominant orbital configuration $^3\Pi$:...$(1\sigma)^2(2\sigma)^1(1\pi_x)^1$ has been derived for the cation. The singlet−triplet energy gap is less sensitive to the methods, which is predicted to be 54, 51, 52, and 53 kcal/mol above the $^1\Sigma^+$ at the CASSCF(4,5), MRMP2, MCQDPT2, and B3LYP levels, respectively. Note that the Ge−H bond lengths amount to 1.598 and 1.654 Å for the singlet and triplet states of the cation, respectively.

In the case of the GeH^- anion, we considered both lower-lying singlet and triplet states whose dominant electronic configurations in the CASSCF(6,5) wave functions are $^3\Sigma^-$: ...$(1\sigma)^2(2\sigma)^2(1\pi_x)^1(1\pi_y)^1$ and $^1\Delta$:...$(1\sigma)^2(2\sigma)^2(1\pi_x)^2(1\pi_y)^0$. CASSCF(6,5)/aug-cc-pVTZ calculations predicted a lower-lying triplet $^3\Sigma^-$ state, which is lying 20 kcal/mol below the singlet $^1\Delta$ state. Nevertheless, in this case, the singlet−triplet gap turns out to be sensitive to the methods. While a comparable gap of 18 kcal/mol has been obtained at the B3LYP level, the state-specific MRMP2 method predicted a larger gap of 24 kcal/mol, and the MCQDPT2 method based on the state-averaged CASSCF reference wave function predicted a markedly smaller gap of 14 kcal/mol. It is clear that in the triplet state, the unpaired electrons occupy each of the degenerate π-MOs, which are having large contributions from the germanium p-orbitals, whereas in the singlet state, only one of these π-MOs is filled, thus giving rise to a multiconfigurational character. The $1\pi \rightarrow 2\pi$ electron jump results in a marginal change in Ge−H bond length, from 1.643 to 1.656 Å at the CASSCF(6,5) level. According to previous studies, DFT methods provide for such species more balanced energetic results.[39] On the basis of the available B3LYP data, we evaluate the electron affinity EA(GeH) = 1.27 eV, the ionization energy IE_a(GeH) = 7.81 eV, and the proton affinity of Ge atom PA(Ge) = 201.3 kcal/mol, with an expected error bar of ±0.15 eV or ±3.0 kcal/mol (cf., Table 5).

B. Ge_2H, Ge_2H^+, and Ge_2H^-. The most recent study on Ge_2H was reported by Wang et al., in which systematic MO calculations were performed.[7] These authors investigated both the linear and the H-bridged isomers of Ge_2H fragment along with an isomerization pathway in the ground state. In the present Article, we rather paid attention to the Ge_2H fragment including a number of excited and charged states. For this purpose, we used the multiconfigurational CASSCF, MRMP2, and MCQDPT2 methods for our search in conjunction with a large aug-cc-pVTZ basis set. In the subsequent sections, the electronic structure of the bridged Ge_2H, its cation, and its anion will be examined.

For CASSCF computations, the 4s and 4p orbitals of Ge and 1s orbital of H are included in the active space, thus leading to a 9 electrons in 9 orbitals active space, referred to hereafter as

TABLE 1: Calculated Total and Relative Energies of the Lowest-Lying Electronic States of GeH, GeH^+, and GeH^- at B3LYP/6-311++G(d,p), CASSCF/aug-cc-pVTZ, MRMP2/aug-cc-pVTZ, and MCQDPT2/aug-cc-pVTZ Levels

			total energy (in au) (relative energy in parentheses in kcal/mol)			
molecule	state	leading orbital configuration	B3LYP/ 6-311++G(d,p)	CASSCF/ aug-cc-pVTZ	MRMP2/ aug-cc-pVTZ	MCQDPT2/ aug-cc-pVTZ
GeH	$^2\Pi$	$...(1\sigma)^2(2\sigma)^2(1\pi_x)^1$	−2077.53725 (0)	−2075.95881 (0)	−2076.02318 (0)	−2076.18234 (0)
	$^4\Sigma$	$...(1\sigma)^2(2\sigma)^1(1\pi_x)^1(1\pi_y)^1$	−2077.45903 (49.1)	−2075.90197 (35.7)	−2075.96188 (38.5)	−2076.11955 (39.4)
GeH^+	$^1\Sigma^+$	$...(1\sigma)^2(2\sigma)^2(1\pi_x)^0$	−2077.25010 (0)	−2075.70967 (0)	−2075.74524 (0)	−2075.90107 (0)
	$^3\Pi$	$...(1\sigma)^2(2\sigma)^1(1\pi_x)^1$	−2077.16542 (53.1)	−2075.62374 (53.9)	−2075.66330 (51.4)	−2075.81706 (52.7)
GeH^-	$^3\Sigma^-$	$...(1\sigma)^2(2\sigma)^2(1\pi_x)^1(1\pi_y)^1$	−2077.58381 (0)	−2075.97177 (0)	−2076.06827 (0)	−2076.22048 (0)
	$^1\Sigma^+$	$...(1\sigma)^2(2\sigma)^2(1\pi_x)^2(1\pi_y)^0$	−2077.55531 (17.9)	−2075.94140 (19.1)	−2076.02979 (24.1)	−2076.19791 (14.2)

TABLE 2: Calculated Total and Relative Energies of Various Lowest-Lying Electronic States of Ge_2H, Ge_2H^+, and Ge_2H^- at B3LYP/6-311++G(d,p), CASSCF/aug-cc-pVTZ, MRMP2/aug-cc-pVTZ, and MCQDPT2/aug-cc-pVTZ Levels

			total (in au) and relative energies (kcal/mol in parentheses)			
molecule	state	leading orbital configuration	B3LYP/6-311++G(d,p)	CASSCF	MRMP2	MCQDPT2
Ge_2H	$^2B_1$	$...(1a_1)^2(2a_1)^2(1b_2)^2(1b_1)^1(3a_1)^2$	−4154.56842 (0)	−4151.40679 (0)	−4151.54719 (0)	−4151.88386 (0)
	$^2A_1$	$...(1a_1)^2(2a_1)^2(1b_2)^2(1b_1)^2(3a_1)^1$	−4154.56252 (3.7)	−4151.40763 (−0.5)	−4151.54887 (−1.05)	−4151.88065 (2.0)
	$^2A'$	$...(1a')^2(2a')^2(3a')^2(1a'')^2(4a')^1$		−4151.39957 (4.5)	−4151.53547 (7.4)	
	$^2\Pi$	$...(1\sigma)^2(2\sigma)^2(3\sigma)^2(1\pi)^2(2\pi)^1$	−4154.55745[a] (6.9)	−4151.39938 (4.7)	−4151.53570 (7.2)	
	$^4A_2$	$...(1a_1)^2(2a_1)^2(1b_2)^2(1b_1)^1(3a_1)^1(2b_2)^1$	−4154.51365 (34.4)	−4151.35771[a] (30.8)	−4151.49664 (31.7)	−4151.82069 (39.6)
	$^4A''$	$...(1a')^2(2a')^2(3a')^2(1a'')^1(4a')^1(5a')^1$	−4154.53234 (22.6)	−4151.37953 (17.1)	−4151.51711 (18.9)	
Ge_2H^+	$^3B_1$	$...(1a_1)^2(2a_1)^2(1b_2)^2(1b_1)^1(3a_1)^1$	−4154.28556 (0)	−4151.16046 (0)	−4151.27307 (0)	−4151.59520 (0)
	$^1A_1$	$...(1a_1)^2(2a_1)^2(1b_2)^2(1b_1)^2(3a_1)^0$	−4154.27300 (7.9)	−4151.15318 (4.6)	−4151.25252 (12.9)	−4151.58030 (9.4)
Ge_2H^-	$^1A_1$	$...(1a_1)^2(2a_1)^2(1b_2)^2(1b_1)^2(3a_1)^2$	−4154.64385 (0)	−4151.45501 (0)	−4151.62310 (0)	−4151.95785 (0)
	$^3A'$	$...(1a')^2, (2a')^2, (3a')^2, (1a'')^2, (4a')^1, (5a')^1$	−4154.60293 (25.7)	−4151.41799 (23.2)	−4151.58748 (22.4)	
	$^3A_2$	$...(1a_1)^2, (2a_1)^2, (1b_2)^2, (1b_1)^1, (3a_1)^2, (2b_2)^1$	−4154.58878[a] (35.6)	−4151.37391 (50.9)	−4151.55206 (44.6)	−4151.89654 (38.5)
	$^3B_2$	$...(1a_1)^2, (2a_1)^2, (1b_2)^2, (1b_1)^0, (3a_1)^2, (2b_2)^1, (1a_2)^1$	−4154.59050 (33.5)	−4151.39778 (35.9)	−4151.57169 (32.3)	−4151.88651 (44.8)

[a] Total energy values are not scaled with zero point energy. The relative energy values are not corrected for ZPE.

CASSCF(9,9). Calculated total energies are listed in Table 2, and the shape of the nine active natural orbitals, labeled under C_{2v} point group, is illustrated in Figure 2.

The leading electronic configurations for the two lowest-lying electronic states of the bridged Ge_2H are $^2B_1$: $...(1a_1)^2(2a_1)^2(1b_2)^2(1b_1)^1(3a_1)^2$ and $^2A_1$:$...(1a_1)^2(2a_1)^2(1b_2)^2(1b_1)^2(3a_1)^1$. The $1b_1$ is a π-bonding MO with respect to the Ge−Ge bond axis, whereas the $3a_1$ orbital corresponds to a σ-bonding MO. The ground state of the bridged Ge_2H fragment, under C_{2v} symmetry, is confirmed to be a $^2B_1$ state. Various optimized geometries for the Ge_2H isomers are included in Figure 3. A quasi-degenerate $^2A_1$ state has been derived at the B3LYP level, being 3.7 kcal/mol above the former. However, CASSCF/aug-cc-pVTZ computations predicted a reversed state ordering with a small energy gap of 0.5 kcal/mol. The CASSCF energy ordering of electronic states is reconfirmed at the MRMP2 level with an energy gap of 1 kcal/mol, employing the same basis set and active space. It is clear from previous studies on similar systems that special care should be taken when dealing with quasi-degenerate electronic states, where often the MRMP2 method could fail.[27,28] In the present system, the MCQDPT2 level predicted the $^2B_1$ state as the ground state, with a $^2B_1-^2A_1$ energy gap of 2.0 kcal/mol.

The geometrical change during this electronic excitation is marginal, as the Ge−Ge and Ge−H bond shrinks by an amount of 0.1 and 0.02 Å, respectively, and the Ge−H−Ge bond angle reduced by ∼3°.

A few electronic states have also been characterized for Ge_2H, of which the C_s $^2A'$ and linear $^2\Pi$ electronic states are among the lowest-lying ones. At the CASSCF/aug-cc-pVTZ level, all evaluated harmonic frequencies for these structures are real values. The bent C_s isomer is energetically 4.5 kcal/mol above the $^2B_1$ by CASSCF(9,9) calculations, but the gap is increased to 7.4 kcal/mol by MRMP2. The SOMO of $^2A'$ is similar to the size and shape of $3a_1$ MO of the ground $^2B_1$. Note that the Ge−Ge and Ge−H bond lengths are reduced considerably as

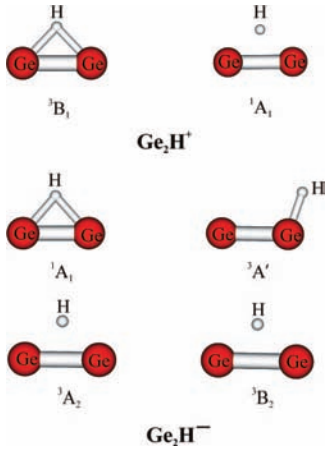

Figure 2. Optimized geometries for the lowest-lying electronic states of Ge_2H^+ using CASSCF(8,9) and Ge_2H^- using CASSCF(10,9) with the aug-cc-pVTZ basis set.

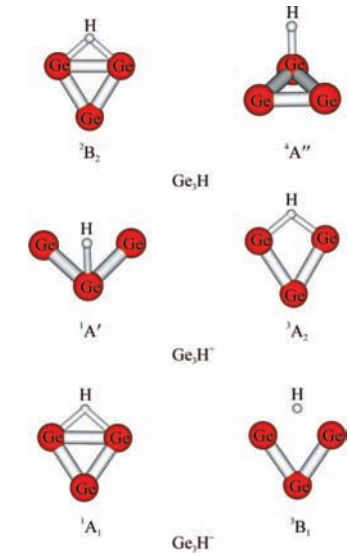

Figure 3. CCSD(T)/aug-cc-pVDZ optimized geometries for the lowest-lying electronic states of Ge_3H, Ge_3H^+, and Ge_3H^- in two different spin manifolds.

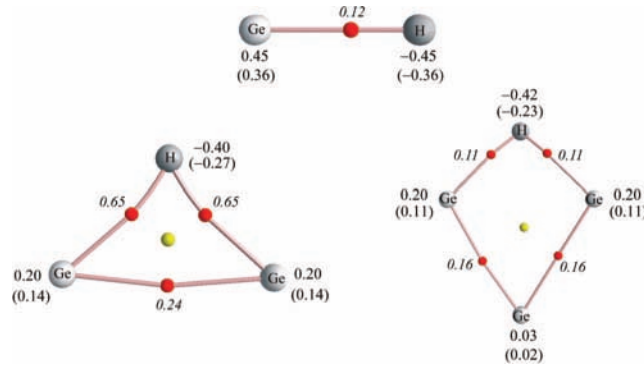

Figure 4. Molecular graphs of the lowest-lying electronic states of GeH, Ge_2H, and Ge_3H. Light gray balls are germanium, and dark gray balls are hydrogen atoms. The ellipticity values of the computed bond critical points are represented in italic numerals along with the NBO charges (within parentheses) and the most accurate AIM-charges on each atom.

compared to those of $^2B_1$. In the linear framework, we were able to derive an isomer in which the unpaired electron occupies the degenerate π-MOs. This $^2\Pi$ state is found 7.2 kcal/mol higher in energy than the ground state at MRMP2 (but 4.7 kcal/mol at CASSCF/aug-cc-pVTZ, Table 2).

In the quartet manifold, a $^4A''$ state (C_s) has been identified. The doublet−quartet energy gap was estimated to be ∼22 kcal/mol at B3LYP, whereas the CASSCF(9,9) and MRMP2 level predicted a smaller gap of ∼18 kcal/mol. The unpaired electrons occupy the 1a″, 4a′, and 5a′ MO's, which are similar in size and shape to the $1b_1$, $4a_1$, and $3a_1$ MO's of the ground state marked under C_{2v} symmetry (cf., Figure 2). These correspond to π- and σ-bonding MO's with respect to the Ge−Ge bond. For $^4A''$, the Ge−Ge bond length is estimated to be 2.509 Å at the CASSCF/aug-cc-pVTZ level, which is larger as compared to the same for the doublet state, with a Ge−Ge−H bond angle of 105.8°.

Another quartet $^4A_2$ state has been found under C_{2v}, which is located at 34 kcal/mol (B3LYP) above the $^2B_1$. A similar gap of ∼32 kcal/mol was predicted by both CASSCF and MRMP2 levels, whereas a larger gap of 39 kcal/mol was obtained by MCQDPT calculations. For this state, the Ge−Ge bond of 2.683 Å is the longest length, and the Ge−H bond is around 1.809 Å (CASSCF(9,9)). The $2b_2$ MO is antibonding with respect to the Ge−Ge bond; therefore, the Ge−Ge elongation can be understood as due to an occupation of an electron in this antibonding MO. However, this structure was characterized as a transition state with one imaginary frequency, which corresponds to in-plane movement of hydrogen atom. Accordingly, the barrier for H-migration $^4A'' \rightarrow {}^4A_2$ amounts to ∼14 kcal/mol in the high spin state. The $^4\Pi$ state derived in the linear geometric manifold was found to be a second-order saddle point in the Ge_2H potential energy surface at CASSCF (9,9) level. The $^4A''-{}^4\Pi$ energy gap is estimated to be ∼16 kcal/mol.

Ionization of Ge_2H results in the formation of a cation for which a triplet state $^3B_1$:...$(1a_1)^2(2a_1)^2(1b_2)^2(1b_1)^1(3a_1)^1$ is the lowest-lying state. Removal of electron is thus more facilitated from an σ-type orbital ($3a_1$). A lower-lying singlet state $^1A_1$: ...$(1a_1)^2(2a_1)^2(1b_2)^2(1b_1)^2$ has been derived for the cation from the quasi-degenerate neutral $^2A_1$. For this cation, we used CASSCF(8,9) wave functions with the same orbitals described above for geometry optimizations. There is considerable change in geometry during the triplet−singlet transition: the Ge−H−Ge bond angle increases by 4.6° and the Ge−Ge bond increases by 0.1 Å. The triplet−singlet $^1A_1-{}^3B_1$ energy gap of Ge_2H^+ is calculated to be sensitive with respect to the methods, 8.0 kcal/mol by B3LYP, 4.6 kcal/mol by CASSCF(8,9), 13.0 kcal/mol by MRMP2, but 9.4 kcal/mol by MCQDPT2.

For the Ge_2H^- anion, CASSCF (10,9) optimized geometries of its different states are illustrated in Figure 4, and their characteristics are described in Table 2. We found a singlet ground state by all methods considered. With a dominant orbital configuration of $^1A_1$:...$(1a_1)^2(2a_1)^2(1b_2)^2(1b_1)^2(3a_1)^2$, this closed-shell state is formed by addition of an electron to the π-type bonding $1b_1$ SOMO of the neutral $^2B_1$ state. This correlates with the fact that the Ge−Ge bond length of 2.350 Å is shorter as compared to that of the neutral ground state. Full occupancy of a bonding orbital with respect to the Ge−Ge bond increases its strength and reduces its length.

In the triplet manifold of the anion, we located a bent (C_s) and two bridged (C_{2v}) structures. The bent structure has a lower-lying state $^3A'$:...$(1a')^2(2a')^2(3a')^2(1a'')^2(4a')^1(5a')^1$. The 4a′ and 5a′ SOMOs have the same size and shape as the $3a_1$ and $2b_2$ counterparts (cf., Figure 2). As compared to the singlet, the Ge−Ge($^3A'$) length is increased by 0.1 Å and the Ge−H bond reduced by 0.16 Å. Two bridged triplet states have the dominant configurations, $^3A_2$:...$(1a_1)^2(2a_1)^2(1b_2)^2(1b_1)^1(3a_1)^2(2b_2)^1$ and $^3B_2$: ...$(1a_1)^2(2a_1)^2(1b_2)^2(1b_1)^1(3a_1)^2(2b_2)^0(1a_2)^1$ as the result from a

TABLE 3: Calculated Total and Relative Energies of the Lowest-Lying Electronic States of Ge_3H, Ge_3H^+, and Ge_3H^- at B3LYP/6-311++G(d,p), CCSD(T)/aug-cc-pVDZ, CCSD(T)/aug-cc-pVTZ, and CCSD(T)/aug-cc-pVQZ Levels

		total (in au) and relative energies (in parentheses in kcal/mol)			
molecule	state	B3LYP/ 6-311++G(d,p)	CCSD(T)/ aug-cc-pVDZ[a]	CCSD(T)/ aug-cc-pVTZ[a]	CCSD(T)/ aug-cc-pVQZ[a]
Ge_3H	$^2B_2$	−6231.61066 (0)	−6226.84676 (0)	−6227.10265 (0)	−6227.12332 (0)
	$^4A''$	−6231.56754 (27.1)	−6226.80460 (26.5)	−6227.05999 (26.8)	−6227.08033 (27)
Ge_3H^+	$^1A'$	−6231.32502 (0)	−6226.566957 (0)	−6226.817787 (0)	−6226.836957 (0)
	$^3A_2$	−6231.31926 (3.6)	−6226.557258 (6.1)	−6226.806798 (6.9)	−6226.825648 (7.1)
Ge_3H^-	$^1A_1$	−6231.69883 (0)	−6226.93270 (0)	−6227.19345 (0)	−6227.21555 (0)
	$^3B_1$	−6231.64487 (33.9)	−6226.879433 (33.4)	−6227.138673 (34.4)	−6227.159863 (34.9)

[a] Total energy values are corrected for ZPE computed at B3LYP level.

$\pi-\pi^*$ excitation. We found that the bent triplet $^3A'$ is lower in energy than the others. The corresponding $^3A'-{}^1A_1$ singlet−triplet energy gap appears to be less-method dependent, being 25 kcal/mol from B3LYP, and 23 and 22 kcal/mol at the CASSCF(10,9) and MRMP2 levels, respectively, in favor of the singlet state. The triplet states $^3A_2$ and $^3B_2$ are found at 38 and 45 kcal/mol above the singlet ground state at the MCQDPT2 level.

On the basis of calculated data, the following thermochemical quantites can be predicted: $IE_a(Ge_2H) = 7.69$ eV, $EA(Ge_2H) = 2.05$ eV, $BDE(Ge_2-H) = 379.2$ kcal/mol, $PA(Ge_2) = 201.7$ kcal/mol, and $HA(Ge_2) = 426.5$ kcal/mol (cf., Table 5).

C. Ge_3H, Ge_3H^+, and Ge_3H^-. For the trigermanium Ge_3H derivatives, the derived electronic states, total, and relative energies are listed in Table 3, and the CCSD(T)/aug-cc-pVDZ optimized geometries are illustrated in Figure 5. Accordingly, our calculations predicted a $^2B_2$ ground state under C_{2v} symmetry. We were also able to identify in the C_s point group a low-lying quartet $^4A''$ state. Both B3LYP and CCSD(T)

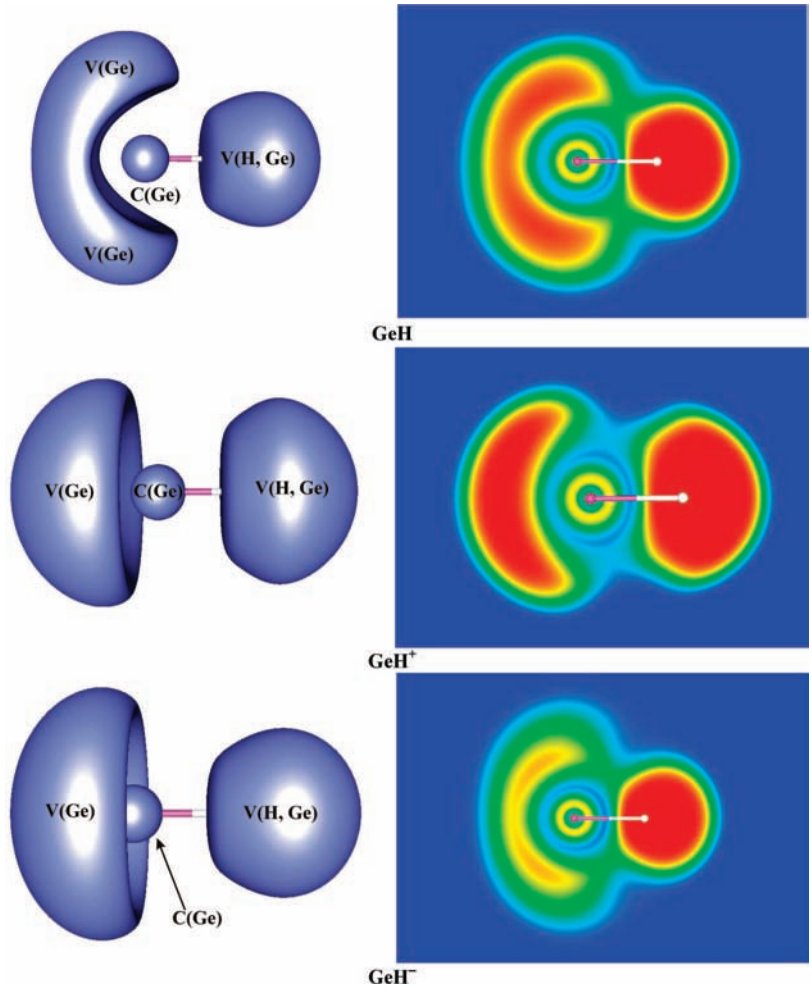

Figure 5. Cut planes and ELF isosurfaces of GeH, GeH^+, and GeH^- ($\eta = 0.7$) at their lowest-lying electronic state (B3LYP/6-311++G(d,p)).

computations result in a doublet−quartet energy gap of 27 kcal/mol. A considerable change in geometry is associated with the doublet−quartet transition, the latter state being nonplanar. For the sake of accuracy, we performed single point energy computations at the CCSD(T)/aug-cc-pVDZ optimized geometries employing the larger aug-cc-pVTZ and aug-cc-pVQZ basis sets (see Table 3 for the total and relative energies).

The Ge_3H^+ cation is characterized by a singlet low-lying state $^1A'$. Geometrically this cation falls under the C_s point group, where the bonded hydrogen atom is situated above the plane containing the three germanium atoms (see Figure 5 for optimized geometries). The B3LYP result is consistent with coupled cluster calculations. The triplet geometry is similar to that of the ground-state $^2B_2$ of the neutral Ge_3H, but with a larger Ge−Ge distance. A triplet $^3A_2$ ground state has been characterized for the C_{2v} cation. We obtained a small singlet−triplet gap of 3.6 kcal/mol by DFT, but a larger gap of 6.1, 6.9, and 7.1 kcal/mol using the coupled cluster CCSD(T) level in conjunction with the aug-cc-pVDZ, TZ, and QZ basis sets, respectively.

CCSD(T) optimized geometries of a few low-lying electronic states of the Ge_3H^- anion are represented in Figure 5, while total and relative energies are listed in Table 3. The anion Ge_3H^- is characterized to have a singlet ground electronic state $^1A_1$. The C_{2v} anion is geometrically similar to the neutral $^2B_2$. Following a triplet excitation, structural change of the anion is not marginal, where the Ge−Ge and Ge−Li bond lengths increase by an amount of 0.1 Å, and the GeGeGe bond angle by 2°. The lowest-lying triplet $^3B_1$ state lies ∼34 kcal/mol above the $^1A_1$ at the DFT level, and 33, 34, and 35 kcal/mol at the CCSD(T) level in conjunction with the aug-cc-pVDZ, TZ, and QZ basis sets, respectively.

Overall, the following thermochemical quantites can be predicted: $IE_a(Ge_3H) = 7.77$ eV, $EA(Ge_2H) = 2.40$ eV, $BDE(Ge_3-H) = 375.9$ kcal/mol, $PA(Ge_3) = 196.6$ kcal/mol, and $HA(Ge_3) = 431.2$ kcal/mol (cf., Table 5).

D. Electronic Structure and Bonding. After establishing the electronic structure of the Ge_nH systems and for a further understanding of the nature of the underlying bonding, we performed a more qualitative analysis of the electron densities making use of the atoms-in-molecules (AIM) and electron localization function (ELF) approaches on some selected systems. Parallel charge computations were also performed adopting the NBO and AIM-charge techniques.

The AIM concept is a useful tool, providing valuable information about the structure and bonding in molecules.[41,42] Accordingly, a critical point (CP), where the gradient of the electron density vanishes, holds chemical information and allows us to define atoms and chemical bonds within a molecule. The wave functions used for AIM analysis were generated at the B3LYP level in conjunction with the 6-311G** basis set using the Gaussian 03 revision D02 suite of programs. The CP's were then located, and the bond paths were plotted using the AIM2000 suite of programs. We have considered three neutral systems for our AIM analysis, GeH, Ge_2H, and Ge_3H. The molecular graphs are illustrated in Figure 6 along with the computed NBO and AIM-charges. The ellipticity, a quantity defined as:

$$\varepsilon = (\lambda_1/\lambda_2 - 1); \lambda_1 \leq \lambda_2 \leq \lambda_3$$

where λ_1, λ_2, and λ_3 are the eigenvalues of the Hessian, measures the behavior of the electron density at a given point, in the plane tangential to the interatomic surface. The ellipticity value ranges from zero to infinity and is widely regarded as a quantitative index of the π-character of the bond. For a complete analysis, the ellipticity values of different critical points are also given in Figure 6.

In the case of Ge−H, we derived three CP's, that is, two attractors and one Ge−H bond critical point (BCP). The ellipticity value of the BCP(Ge−H) is 0.12, and the computed NBO charges suggest a certain positive charge on the germanium atom (0.36 e) and a negative charge on the hydrogen (−0.36 e). The computed AIM-charges show the same trend, amounting to 0.45 e on Ge and −0.45 e on H.

For Ge_2H, the molecular graph contains three BCP's (two Ge−H plus one Ge−Ge) and one Ge−Ge−H ring critical point (RCP). The ellipticity value for the BCP(Ge−H) amounts to 0.65, whereas that for Ge−Ge is 0.24. The computed NBO charges suggest an obvious negative charge on H (0.27 e) with small positive charges on the Ge atoms (0.14 e each). This is indeed confirmed by the AIM-charges, which give however larger values (−0.40 e on H and 0.20 e on each Ge). The molecular graph of Ge_2H turns out to be different from that of Ge_2Li,[27] where the latter lacks a Ge−Ge−Li RCP, but more similar in that respect to the situation of the Ge_2Cr cluster.[29]

In Ge_3H, the computed molecular graph contains 4 BCP's (two Ge−H and two Ge−Ge) and one Ge−Ge−Ge−H RCP. Interestingly, this structure lacks a Ge−Ge BCP and a Ge−Ge−Ge RCP. The topology of the electron density of Ge_3H is thus completely different from that of Ge_3Li,[28] which has three BCP(Ge−Ge), one RCP(Ge−Ge−Ge), plus one BCP(Ge−Li). It is also at variance with Ge_3Cr,[29] which has three BCP(Ge−Ge), two BCP(Ge−H), one RCP(Ge−Ge−Ge), and one RCP(Ge−Ge−H). It is clear from the above analysis that the topologies of the electron density for the germanium monohydrides differ much from those of the lithium-doped and chromium-doped counterparts.

Similar to GeH and Ge_2H, there is an obvious electron transfer to the hydrogen atom from the germanium unit. The NBO charge amounts to −0.23 e, while a larger value of −0.42 e is predicted by AIM. In view of this apparent electron transfer, it can be concluded that it is a $Ge_n^+H^-$ ($n = 1, 2, 3$) interaction. The ellipticity values of various BCP's are illustrated in Figure 6.

For additional insights, we performed an ELF analysis on some molecules under consideration. The ELF is a simple measure of the electron localization in atomic and molecular systems.[43] The ELF values are always in a range of [0;1] and relatively large where the electrons are unpaired or formed into pairs with antiparallel spins. The zero flux surfaces of the ELF separate the electron density space into basins (Ω_i), thus helping us define and calculate the properties of core, chemical bond, and lone pairs.[43] The corresponding basins are mainly classified into two types, core and valence basins. While the former are mainly located around the nuclei and always occur when the atomic number is larger than 2, the latter are characterized by their synaptic orders, that is, the number of the core basins that share a common boundary surface with the valance basin. Monosynaptic basins represent the lone pairs, and the disynaptic basins belong to the covalent bonds. The integral of the electron density over Ω_i shows the population of the given basin.

The calculations were performed using the TopMod suites of programs, and the ELF isosurfaces were visualized using the gOpenMOL software.[44] The ELF isosurfaces and their cut planes of GeH, GeH^+, and GeH^- are illustrated in Figure 1S, while those of Ge_2H, Ge_2H^+, and Ge_2H^- are illustrated in Figure 2S. The mean electron populations computed for the basins localized for each molecule are summarized in Table 4. In the case of Ge−H, we located three type of basins, that is, the germanium core basin C(Ge), and the valence basins including one V(H,Ge)

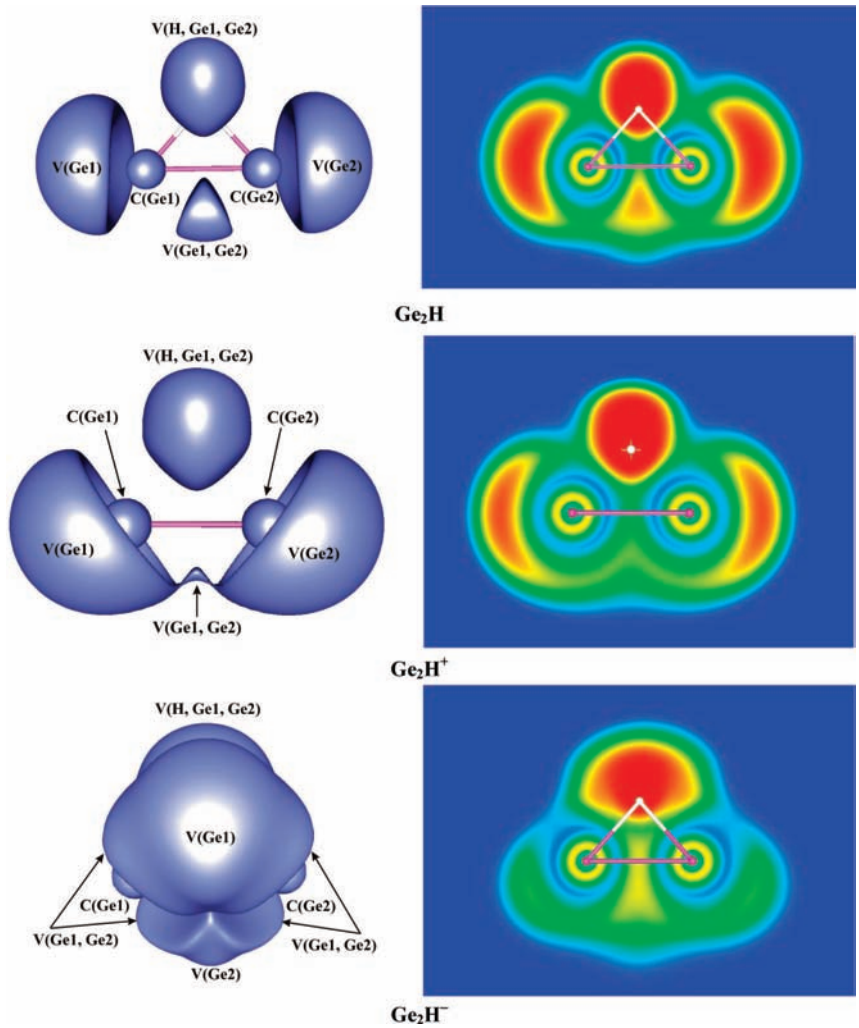

Figure 6. Cut planes and ELF isosurfaces of Ge_2H, Ge_2H^+, and Ge_2H^- ($\eta = 0.7$) at their ground electronic state (B3LYP/6-311++G(d,p)).

TABLE 4: Mean Electronic Populations Computed for Basins Localized in Neutral Ge_nH ($n = 1, 2$), Cations, and Anions (B3LYP/6-311++G(d,p))

	basins						
molecule	C(Ge1)	C(Ge2)	V(H, Ge)	V(H, Ge1, Ge2)	V(Ge1, Ge2)	V(Ge1)	V(Ge2)
GeH	27.63		2.07			1.64	
GeH^+	27.61		2.19			2.19	
GeH^-	27.61		2.21			4.12	
Ge_2H	27.61	27.61		2.00	2.74	2.51	2.51
Ge_2H^+	27.56	27.56		2.11	0.64	3.06	3.06
Ge_2H^-	27.56	27.56		2.41	1.47	1.39	1.39

TABLE 5: Calculated Ionization Energy (IE), Electron Affinity (EA), and Protonation Affinity (PA) of Different Molecules Considered at B3LYP/6-311++G(d,p) Level

property in kcal/mol (eV in parentheses)	molecule					
	GeH	Ge_2H	Ge_3H	Ge	Ge_2	Ge_3
IE	180.2 (7.81)	177.5 (7.69)	179.2 (7.77)			
EA	29.2 (1.27)	47.3 (2.05)	55.3 (2.40)			
PA				201.3	201.7	196.6

and two V(Ge). The mean electron population in the V(H,Ge) basin amounts to 2.07 electrons, while that of the V(Ge) amounts to 1.64 electrons. It can be concluded that the V(Ge) basins are mainly the Ge lone pairs. The shape of basins present in the GeH^+ and GeH^- is different from that in the neutral molecule. In the cation, the occurrence of three types of basins is similar to that in the neutral, C(Ge), V(H,Ge), and V(Ge). However, we were able to locate only one V(Ge) basin in GeH^+ having a mean electronic population of 2.19 electrons. Note that in the neutral molecule, two such basins were located with a total electronic population of 3.28 electrons. Thus, during the formation of the cation, removal of electron is facilitated from the Ge lone pair electrons. The total electronic population of the V(H,Ge) basin in GeH^- amounts to 2.21 electrons, while it

is 4.12 electrons for the V(Ge) basin. This indicates that formation of the anion arises from an additional electron on the lone pair basin V(Ge).

In Ge_2H, our computations derived the following basins: the monosynaptic core basins C(Ge1), C(Ge2); the monosynaptic valence (Ge1), V(Ge2); the disynaptic valence V(Ge1, Ge2); and a trisynaptic valence V(H,Ge1,Ge2) basin. Again, the topology of the ELF for Ge_2H turn thus out to be different from that of Ge_2Li[27] and Ge_2Cr.[29] Occurance of the trisynaptic basin V(H,Ge1,Ge2) clearly suggests a certain Ge−H−Ge three center bond in the molecule. The mean population of this basin is 2 electrons. The V(Ge) basins, which are mainly the Ge lone pair, have a population of 2.5 electrons each. The disyanaptic V(Ge1,Ge2) basin has a population of 2.7 electrons.

For Ge_2H^+, the same number of basins were identified as in the neutral molecule, that is, C(Ge1), C(Ge2), V(Ge1), V(Ge2), V(Ge1,Ge2), and V(H,Ge1,Ge2). They differ from each other mainly in shape and populations. Note that the V(Ge1, Ge2) population is now 0.6 electrons and V(Ge) basins have 3.1 electrons each. Such a change shows that, upon ionization, the electron removal occurs from the V(Ge1,Ge2) basin (∼2 electrons), followed by increase in the V(Ge) basin population (∼1 electron). The emergence of the trisynaptic basin V(H,Ge1,Ge2) again points out a three-center bonding interaction between the hydrogen and the germanium unit.

The ELF isosurface of the Ge_2H^- anion is entirely different in size and shape from that of the neutral and cationic counterparts. The basins localized in Ge_2H^- include C(Ge1), C(Ge2), V(Ge1), V(Ge2), four V(Ge1,Ge2), and one V(H,Ge1,Ge2). The V(H,Ge1,Ge2) basin is again present in the anion with a mean population of 2.4 electrons, consistent with the presence of a three-center bond. The main difference in the ELF topology of the anion lies in the fact that it possesses four V(Ge1,Ge2), whereas there is only one V(Ge1,Ge2) in either the neutral or the cation. In Ge_2H, the total population on these four V(Ge1,Ge2) basins amounts to 5.9 electrons. The V(Ge) population is considerably reduced from the 2.5 electrons value of the neutral to 1.4 electrons. Comparing the basin populations of Ge_2H and its anion, it seems reasonable to conclude that the additional electron is located in the V(Ge1,Ge2) basin. The ELF topology also suggests that the germanium lone pair V(Ge) contributes considerably toward the Ge−Ge bonding.

Concluding Remarks

We have applied quantum chemical methods to investigate the electronic structure of germanium monohydrides, Ge_nH, with *n* ranging from 1 to 3, in the neutral, cationic, and anionic states. From the computed results, the following conclusions can be drawn: (i) for all germanium monohydrides considered, a low-spin electronic ground state is predicted; (ii)the singlet−triplet and doublet−quartet energy gaps predicted using the B3LYP functional are in agreement with the higher level MO results; (iii) for Ge_3H, a doublet $^2B_2$ state has been derived as the ground electronic state, based on CCSD(T) computations, with a doublet−quartet energy gap of ∼27 kcal/mol; (iv) in the cation Ge_3H^+ and anion Ge_3H^-, the closed-shell singlet states are derived, that is, $^1A'$ and $^1A_1$, respectively, as the lowest-lying states; the singlet triplet energy gap is estimated to be 6 kcal/mol for the cation and a larger gap of ∼34 kcal/mol for the anion; (v) the AIM analysis suggests that the topology of the electron density in germanium monohydrides is entirely different from that of the lithium-doped counterparts; (vi) NBO and AIM-charges on GeH, Ge_2H, and Ge_3H show a certain positive net charge on the germanium unit, indicating a considerable charge transfer to the H atom leading to a $Ge_n^+H^-$ polarization; (vii) in Ge_2H, the ELF analysis points out that the Ge−H bond is predominantly a three-center-two-electron bond, and (viii) due to the large BDE(Ge_nH), PA, and HA affinities, it seems that the Ge_3 cluster could capture a hydrogen atom in whatever charge state, leading to a stable entity.

Acknowledgment. We are indebted to the Flemish Fund for Scientific Research (FWO-Vlaanderen) and the KULeuven Research Council (GOA and IDO programs and doctoral scholarship) for continuing financial support.

Supporting Information Available: Shape of the natural orbitals, and Cartesian coordinates of different molecules considered. This material is available free of charge via the Internet at http://pubs.acs.org.

References and Notes

(1) Li, C.; John, S.; Banerjee, S. *J. Electron. Mater.* **1995**, *24*, 875.
(2) Grev, R. S.; Deleeuw, B. J.; Schaefer, H. F., III *Chem. Phys. Lett.* **1990**, *165*, 257. Trinquier, G. *J. Am. Chem. Soc.* **1990**, *112*, 2130. Grev, R. S. *Adv. Organomet. Chem.* **1991**, *33*, 125.
(3) Becerra, R.; Boganov, S. E.; Egorov, M. P.; Faustov, V. I.; Nefdov, O. M.; Walsh, R. *J. Am. Chem. Soc.* **1998**, *120*, 12657.
(4) Jackson, P.; Sandig, N.; Diefenbach, M.; Schroeder, D.; Schwarz, H.; Srinivas, R. *Chem.-Eur. J.* **2001**, *7*, 151. Antoniotti, P.; Operti, L.; Rabezzana, R.; Vaglio, G. A.; Guarini, A. *Rapid Commun. Mass Spectrom.* **2002**, *16*, 185.
(5) Ricca, A.; Bauschlicher, C. W., Jr *J. Phys. Chem. A* **1999**, *103*, 11121.
(6) Antoniotti, P.; Operti, L.; Rabezzana, R.; Vaglio, G. A. *J. Mol. Struct. (THEOCHEM)* **2003**, *663*, 1.
(7) Wang, H.; Wang, S.; Yamaguchi, Y.; Schaefer, H. F., III *J. Chem. Phys.* **2006**, *125*, 164317.
(8) Koizumi, H.; Dávalos, J. Z.; Baer, T. *Chem. Phys.* **2006**, *324*, 385.
(9) Jarrold, M. F. *Science* **1991**, *252*, 1085.
(10) Raghavachari, K.; Curtiss, L. A. *Quantum Mechanical Electronic Structure Calculations with Chemical Accuracy*; 1995.
(11) Kohl, V. G. *Z. Naturforsch.* **1954**, *9A*, 913.
(12) Arnold, C. C.; Xu, C.; Burton, G. R.; Neumark, D. M. *J. Chem. Phys.* **1995**, *102*, 6982.
(13) Burton, G. R.; Xu, C.; Arnold, C.; Neumark, D. M. *J. Chem. Phys.* **1996**, *104*, 2757. Burton, G. R.; Xu, C.; Neumark, D. M. *Surf. Rev. Lett.* **1996**, *3*, 383.
(14) Cheshnovsky, O.; Yang, S. H.; Pettiette, C. L.; Craycraft, M. J.; Liu, Y.; Smalley, R. E. *Chem. Phys. Lett.* **1987**, *138*, 119.
(15) Gingerich, K. A.; Finkbeiner, H. C.; Schmude, R. W., Jr *J. Am. Chem. Soc.* **1994**, *116*, 3884. Gingerish, K. A.; Shim, I.; Guptha, S. K.; Kingcade, J. E. *Surf. Sci.* **1985**, *156*, 495.
(16) Kingcade, J. E.; Choudary, U. V.; Gingerish, K. A. *Inorg. Chem.* **1979**, *18*, 3094.
(17) Negishi, Y.; Kawamata, H.; Hayase, T.; Gomei, M.; Kishi, R.; Hayakawa, F.; Nakajima, A.; Kaya, K. *Chem. Phys. Lett.* **1997**, *269*, 199.
(18) Xu, C.; Taylor, T. R.; Burton, G. R.; Neumark, D. M. *J. Chem. Phys.* **1998**, *108*, 1395.
(19) Jackson, P.; Fisher, K. J.; Gadd, G. E.; Dance, I. G.; Smith, D. R.; Willett, G. D. *Int. J. Mass Spectrom. Ion Processes* **1997**, *164*, 45.
(20) Dai, D.; Balasubramanian, K. *J. Chem. Phys.* **1996**, *105*, 5901.
(21) Balasubramanian, K. *Chem. Rev.* **1990**, *90*, 93.
(22) Dixon, D. A.; Gole, J. L. *Chem. Phys. Lett.* **1992**, *188*, 560.
(23) Lanza, G.; Millefiori, S.; Millefiori, A. *J. Chem. Soc., Faraday Trans.* **1993**, *89*, 2961.
(24) Archibong, E. F.; St-Amant, A. *J. Chem. Phys.* **1998**, *109*, 962.
(25) Deutsch, P. W.; Curtiss, L. A.; Blaudeau, J. P. *Chem. Phys. Lett.* **1997**, *270*, 413.
(26) Ogut, S.; Chelikowsky, J. R. *Phys. Rev. B* **1997**, *55*, R4914.
(27) Gopakumar, G.; Lievens, P.; Nguyen, M. T. *J. Chem. Phys.* **2006**, *124*, 214312.
(28) Gopakumar, G.; Lievens, P.; Nguyen, M. T. *J. Phys. Chem. A* **2007**, *111*, 5353.
(29) Hou, X.-J.; Gopakumar, G.; Lievens, P.; Nguyen, M. T. *J. Phys. Chem. A* **2007**, *111*, 13544.
(30) Schmidt, M. W.; Gordon, M. S. *Annu. Rev. Phys. Chem.* **1998**, *49*, 233.
(31) Nakano, H. J. *Chem. Phys. Lett.* **1993**, *99*, 7983.
(32) Hirao, K. *Chem. Phys. Lett.* **1992**, *196*, 397. Hirao, K. *Chem. Phys. Lett.* **1992**, *190*, 374. Hirao, K. *Chem. Phys. Lett.* **1993**, *201*, 59.

(33) Brandow, B. H. *Int. J. Quantum Chem.* **1979**, *15*, 207. Brandow, B. H. *Rev. Mod. Phys.* **1967**, *39*, 771. Schucan, T. H.; Weidenmuller, H. *Ann. Phys.* **1972**, *73*, 108. Schucan, T. H.; Weidenmuller, H. *Ann. Phys.* **1973**, *76*, 483. Witek, H. A.; Choe, Y. K.; Finley, J. P.; Hirao, K. J. *J. Comput. Chem.* **2002**, *23*, 957.

(34) Frisch, M. J.; Trucks, G. W.; Schlegel, H. B.; Scuseria, G. E.; Robb, M. A.; Cheeseman, J. R.; Montgomery, J. A., Jr.; Vreven, T.; Kudin, K. N.; Burant, J. C.; Millam, J. M.; Iyengar, S. S.; Tomasi, J.; Barone, V.; Mennucci, B.; Cossi, M.; Scalmani, G.; Rega, N.; Petersson, G. A.; Nakatsuji, H.; Hada, M.; Ehara, M.; Toyota, K.; Fukuda, R.; Hasegawa, J.; Ishida, M.; Nakajima, T.; Honda, Y.; Kitao, O.; Nakai, H.; Klene, M.; Li, X.; Knox, J. E.; Hratchian, H. P.; Cross, J. B.; Bakken, V.; Adamo, C.; Jaramillo, J.; Gomperts, R.; Stratmann, R. E.; Yazyev, O.; Austin, A. J.; Cammi, R.; Pomelli, C.; Ochterski, J. W.; Ayala, P. Y.; Morokuma, K.; Voth, G. A.; Salvador, P.; Dannenberg, J. J.; Zakrzewski, V. G.; Dapprich, S.; Daniels, A. D.; Strain, M. C.; Farkas, O.; Malick, D. K.; Rabuck, A. D.; Raghavachari, K.; Foresman, J. B.; Ortiz, J. V.; Cui, Q.; Baboul, A. G.; Clifford, S.; Cioslowski, J.; Stefanov, B. B.; Liu, G.; Liashenko, A.; Piskorz, P.; Komaromi, I.; Martin, R. L.; Fox, D. J.; Keith, T.; Al-Laham, M. A.; Peng, C. Y.; Nanayakkara, A.; Challacombe, M.; Gill, P. M. W.; Johnson, B.; Chen, W.; Wong, M. W.; Gonzalez, C.; Pople, J. A. Gaussian 03, revision C.01; Gaussian, Inc.: Wallingford, CT, 2004.

(35) Schmidt, M. W.; Baldridge, K. K.; Boatz, J. A.; Elbert, S. T.; Gordon, M. S.; Jensen, J. H.; Koseki, S.; Matsunaga, N.; Nguyen, K. A.; Su, S. J.; Windus, T. L.; Dupuis, M.; Montgomery, J. A. *J. Comput. Chem. Phys.* **1993**, *14*, 1347; GAMESS program.

(36) Biegler-König, F.; Schönbohm, J.; Bayles, D. *J. Comput. Chem.* **2001**, *22*, 545; AIM2000−A Program to Analyze and Visualize Atoms in Molecules.

(37) Henkelman, G.; Arnaldsson, A.; Jónsson, H. *Comput. Mater. Sci.* **2006**, *36*, 254. Sanville, E.; Kenny, S. D.; Smith, R.; Henkelman, G. *J. Comput. Chem.* **2007**, *28*, 899.

(38) Noury, S.; Krokidis, X.; Fuster, F.; Silvi, B. *Comput. Chem.* **1999**, *23*, 604. Matito, E.; Silvi, B.; Duran, M.; Sola, M. *J. Chem. Phys.* **2006**, *125*, 024301.

(39) Li, Q.-S.; Lü, R.-H.; Xie, Y.; Schaefer, H. F., III *J. Comput. Chem.* **2002**, *23*, 1642.

(40) Huber, K. P.; Herzberg, G. *Constants of Diatomic Molecules*; Van Nostrand: New York, 1979.

(41) Bader, R. F. *Atoms in Molecules A Quantum Theory*; Oxford University Press: New York, 1995.

(42) Popellier, P. *Atoms in Molecules An Introduction*; Prentice Hall: New York, 2000.

(43) Becke, A. D.; Edgecombe, K. E. *J. Chem. Phys.* **1990**, *92*, 5397. Silvi, B.; Savin, A. *Nature* **1994**, 683.

(44) Laaksonen, L. J. *J. Mol. Graphics* **1992**, *10*, 33. Bergman, D. L.; Laaksonen, L.; Laaksonen, A. *J. Mol. Graphics Modell.* **1997**, *15*, 301.

JP805173N